STEM CELLS®

TRANSLATIONAL AND CLINICAL RESEARCH

TNF-Stimulated Gene-6 Is a Key Regulator in Switching Stemness and Biological Properties of Mesenchymal Stem Cells

BARBARA ROMANO,[a,*] SUDHARSHAN ELANGOVAN,[b,c,*] MARCO ERRENI,[d] EMANUELA SALA,[c] LUCIANA PETTI,[c] PAOLO KUNDERFRANCO,[e] LUCA MASSIMINO,[f] SILVIA RESTELLI,[b,c] SHRUTI SINHA,[g] DONATELLA LUCCHETTI,[h] ACHILLE ANSELMO,[i] FEDERICO SIMONE COLOMBO,[i] MATTEO STRAVALACI,[b,j] VINCENZO ARENA,[k] SILVIA D'ALESSIO,[b,c] FEDERICA UNGARO,[b,c] ANTONIO INFORZATO,[b,j] ANGELO A. IZZO,[a] ALESSANDRO SGAMBATO,[h] ANTHONY J. DAY,[l] STEFANIA VETRANO [b,c]

ABSTRACT

Mesenchymal stem cells (MSCs) are well established to have promising therapeutic properties. TNF-stimulated gene-6 (TSG-6), a potent tissue-protective and anti-inflammatory factor, has been demonstrated to be responsible for a significant part of the tissue-protecting properties mediated by MSCs. Nevertheless, current knowledge about the biological function of TSG-6 in MSCs is limited. Here, we demonstrated that TSG-6 is a crucial factor that influences many functional properties of MSCs. The transcriptomic sequencing analysis of wild-type (WT) and TSG-6$^{-/-}$-MSCs shows that the loss of TSG-6 expression leads to the perturbation of several transcription factors, cytokines, and other key biological pathways. TSG-6$^{-/-}$-MSCs appeared morphologically different with dissimilar cytoskeleton organization, significantly reduced size of extracellular vesicles, decreased cell proliferative rate, and loss of differentiation abilities compared with the WT cells. These cellular effects may be due to TSG-6-mediated changes in the extracellular matrix (ECM) environment. The supplementation of ECM with exogenous TSG-6, in fact, rescued cell proliferation and changes in morphology. Importantly, TSG-6-deficient MSCs displayed an increased capacity to release interleukin-6 conferring pro-inflammatory and pro-tumorigenic properties to the MSCs. Overall, our data provide strong evidence that TSG-6 is crucial for the maintenance of stemness and other biological properties of murine MSCs. STEM CELLS *2019;37:973–987*

SIGNIFICANCE STATEMENT

Mesenchymal stem cells (MSCs) are a heterogeneous population of pluripotent stem cells that are difficult to study due to the lack of specific markers. Isolation, culture, and in vitro manipulation may influence the expansion of a selective clonal population exhibiting specific functions. Moreover, heterogeneity and lack of predictive biomarkers of their efficacy widely impact the translational use of MSCs. TNF-stimulated gene-6 (TSG-6), acting as an autocrine factor regulating morphology and several other key cellular processes, is crucial for the maintenance of stemness and biological properties of MSCs. Its loss is associated with the abrogation of immunomodulatory activities and leads to a pro-tumorigenic phenotype. These observations warrant further investigations with human MSCs and pave the way for TSG-6 being used as a predictive marker for the success of MSC-based therapy.

INTRODUCTION

Mesenchymal stem cells (MSCs) are a heterogeneous population of adult stem/stromal cells isolated from easily accessible sources including bone marrow, adipose tissue, and umbilical cord with the multipotency capability to differentiate into various cell lineages (reviewed in [1, 2]). The potent immunoregulatory and regenerative properties exerted by MSCs [3–6], and their lack of immunogenicity [7] have attracted growing interest in the treatment of autoimmune, degenerative, and inflammatory disorders. The overwhelming evidence of the beneficial features of MSCs has led to the exponential increase, in the last decade, of the number of registered clinical trials on MSC-based therapy (ClinicalTrials.gov). However, only a few of them have successfully reached the final phases of development. The discrepancy between the promising therapeutic properties of MSCs in experimental models and their current clinical effectiveness might be attributed in part to the heterogeneity of these cells [8] leading to their variability in terms of quality and efficacy. Moreover, their therapeutic utility has been limited because of the absence of a specific predictive marker of their activity.

[a]Department of Pharmacy, School of Medicine and Surgery, University of Naples Federico II, Naples, Italy; [b]Department of Biomedical Sciences, Humanitas University, Pieve Emanuele, Milan, Italy; [c]IBD Center, Laboratory of Gastrointestinal Immunopathology, Humanitas Clinical and Research Center—IRCCS, Rozzano, Milan, Italy; [d]Unit of Advanced Optical Microscopy, Humanitas Clinical and Research Center—IRCCS, Rozzano, Milan, Italy; [e]Bioinformatic Unit, Humanitas Clinical and Research Center—IRCCS, Rozzano, Milan, Italy; [f]Stem Cell and Neurogenesis Unit, Division of Neuroscience, San Raffaele Scientific Institute, Milan, Italy; [g]Genome Biology Unit, Istituto Nazionale di Genetica Molecolare "Romeo ed Enrica Invernizzi" (INGM), Milan, Italy; [h]Institute of General Pathology, Fondazione Policlinico Universitario Agostino Gemelli IRCCS-Catholic University, Rome, Italy; [i]Flow Cytometry Core, Humanitas Clinical and Research Center, Rozzano, Italy; [j]Department of Immunology and Inflammation, Humanitas Clinical and Research Center—IRCCS, Rozzano, Milan, Italy; [k]Area of Pathology, Department of Woman and Child Health and Public Health, Fondazione Policlinico Universitario A. Gemelli-IRCCS; [l]Wellcome Trust Centre for Cell-Matrix Research and Lydia Becker Institute of Immunology and Inflammation, Faculty of Biology, Medicine, & Health, University of Manchester, Manchester Academic Health Science Centre, Manchester, United Kingdom

[*]Contributed equally.

Correspondence: Stefania Vetrano, Ph.D., Department of Biomedical Sciences, Humanitas University, Via Rita Levi Montalcini, 20090 Pieve Emanuele, Milan, Italy. Telephone: 39-0282245148; e-mail: stefania.vetrano@humanitasresearch.it

Received October 5, 2018; accepted for publication February 22, 2019; first published online April 3, 2019.

http://dx.doi.org/10.1002/stem.3010

Although the clinical use of MSCs has shown an excellent safety profile to date [9, 10], the pro-tumorigenic effects of various MSC populations [11–13] have not been fully explored, which is needed if MSCs are to reach their full clinical potential. Therefore, there is an urgent, unmet clinical need for biomarkers able to predict MSC efficacy and off-target effects before transplantation into clinical practice. Murine MSCs, despite major differences compared with human MSCs [14, 15], can serve as a useful tool to explore characteristic biological properties, or indeed molecules that may be useful as potential biomarkers to predict their therapeutic activities.

Tumor necrosis factor-stimulated protein 6 (TNFAIP6 or TNF-stimulated gene-6 [TSG-6]) is an ~35 kDa secreted protein produced by immune cells (e.g., neutrophils, monocytes, macrophages, myeloid dendritic cells) and by stromal cells (e.g., fibroblasts and smooth muscle cells) often in response to pro-inflammatory mediators including TNF-α and interleukin (IL)-1β [16–18]. TSG-6 exerts strong anti-inflammatory properties, acting as a potent inhibitor of neutrophil migration, suppressing inflammatory signaling, and contributing to the downregulation of the protease network. This wide functional repertoire appears to be correlated, at least in part, with TSG-6's capacity to regulate matrix organization/function [18]. For example, TSG-6 has the potential to tune the mechanical properties of the matrix [19, 20], which can influence the association of the ubiquitous polysaccharide hyaluronan (HA) with its cell surface receptors [20–22] and communicate anti-inflammatory signals to the cell [23]. Moreover, TSG-6 modulates the interaction of chemokines with heparan sulfate on the cell surface and in the matrix [24, 25] and thus the bioavailability of these important extracellular signaling molecules [18]. Increasing evidences has demonstrated that TSG-6 is secreted by MSCs and is responsible for a significant part of their beneficial effects. Indeed, murine and human MSCs where the expression of TSG-6 has been reduced (e.g., by siRNA), failed to resolve inflammatory conditions [18, 26–30] displaying a loss of their immunosuppressive activities. However, whether the lack of TSG-6 leads to further changes in the functions of MSCs remains to be investigated.

Here, we identify TSG-6 as having a crucial role in regulating stemness and directing the biological properties of murine MSCs.

Materials and Methods

Animals

Mice were housed at the specific-pathogen-free animal house of Humanitas Clinical Research Center (Italy). MSCs were isolated from bone marrow of 4-week-old to 6-week-old male/female mice of Balb/c TSG-6$^{-/-}$ (C.129S6-Tnfaip6tm1Cful/J; The Jackson Laboratory, Paris, France) and wild-type (WT) littermate mice. Total splenocytes were isolated from the spleen of Balb/c WT mice. The colorectal cancer (CRC) model associated with inflammation was induced in 8-week-old to 12-week-old female C57BL/6 mice, whereas the xenograft model of CRC was induced in athymic nude 8-week-old female mice (both purchased at The Jackson Laboratory). All the procedures were in conformity with the principles of laboratory animal care, in compliance with national (*Direttiva 2010/63/UE*) laws and policies and approved by the Italian Ministry of Health. Other experimental procedures are detailed in the Supporting Information.

Results

Loss of TSG-6 Affects the Morphology of MSCs

In order to explore whether and how TSG-6 influences MSC biological functions and activities, MSCs were isolated from the bone marrow of TSG-6$^{-/-}$-mice and WT-mice and characterized as previously described [30] by flow cytometry. Although TSG-6$^{-/-}$-MSCs differed in size scatter height (SSC-H) and forward scatter (FSC) from WT cells (Fig. 1A), both groups of cells displayed the typical immunophenotype of bona fide MSCs lacking expression of hematopoietic markers (CD45 and CD117), the prototypical endothelial marker CD31, and expressing stemness markers, such as stem cells antigen (SCA)-1, as well as markers reported to be highly expressed on MSCs including CD106, CD29, and CD44 (Fig. 1A). However, the expression of SCA-1 and CD44 appeared reduced in TSG-6$^{-/-}$-MSCs as compared with WT MSCs (Fig. 1A).

Next, we studied the transcriptome of two different clones of WT-MSCs and three different clones of TSG-6$^{-/-}$-MSCs by RNA sequencing (RNAseq) analysis. Despite intragroup variability (i.e., across clones with the same genotype), principal component analysis and hierarchical clustering clearly separated WT-MSCs from TSG-6$^{-/-}$-MSCs (Fig. 1B, 1C). Overall 1,537 downregulated and 1,487 upregulated genes were identified in TSG-6$^{-/-}$-MSCs compared with their WT counterparts (false discovery rate (FDR) < 0.1; Fig. 1C). Loss of the TSG-6 gene affected pathways related to many biological processes, as shown by the gene set enrichment analysis (GSEA) summary ($p < .001$). Particularly, we noticed significant changes in gene sets related to cell organization, cell cycle, immune response, and cell metabolism (Fig. 1D). Furthermore, investigations by Ingenuity Pathway Analysis (IPA) confirmed a significant modulation in genes involved in cell cycle, cell death and survival, cell morphology, cellular movement, DNA replication, and repair (Fig. 2A). In order to analyze the effect of TSG-6 deletion on protein expression, we selected the top seven differential genes (Sox2, Areg, Mmp3, Dnm1, Pxn, HoxB7, and Acta2; $p < .001$) from the RNAseq comparison of TSG-6$^{-/-}$-MSCs and WT-MSCs (Supporting Information Fig. S1A), and quantified their protein levels by Western blot or immunofluorescence assay. The level of proteins encoded by Sox2, Mmp3, Dmn1, Pxn, and Areg were significantly downregulated, whereas those encoded by HoxB7 and Acta2 were upregulated in TSG-6$^{-/-}$-MSCs compared with WT-MSCs (Supporting Information Fig. S1B–S1D), thus consistent with the results of RNA sequencing. Interestingly, the decreased expression of paxillin, a scaffold protein encoded by Pxn and involved in the interaction of sites of cell adhesion to the extracellular matrix (ECM) and in the regulation of actin polymerization [31], suggested a defective actin organization in absence of TSG-6.

GSEA analysis performed on the cytoskeletal gene set revealed a significant decrease in the enrichment score across the genes in TSG-6$^{-/-}$-MSCs compared with WT-MSCs, supporting a different cytoskeletal organization in the two groups of cells (Fig. 2B). Morphologically, WT-MSCs appeared to be more elongated and crescent-shaped than TSG-6$^{-/-}$-MSCs (Fig. 2C), which

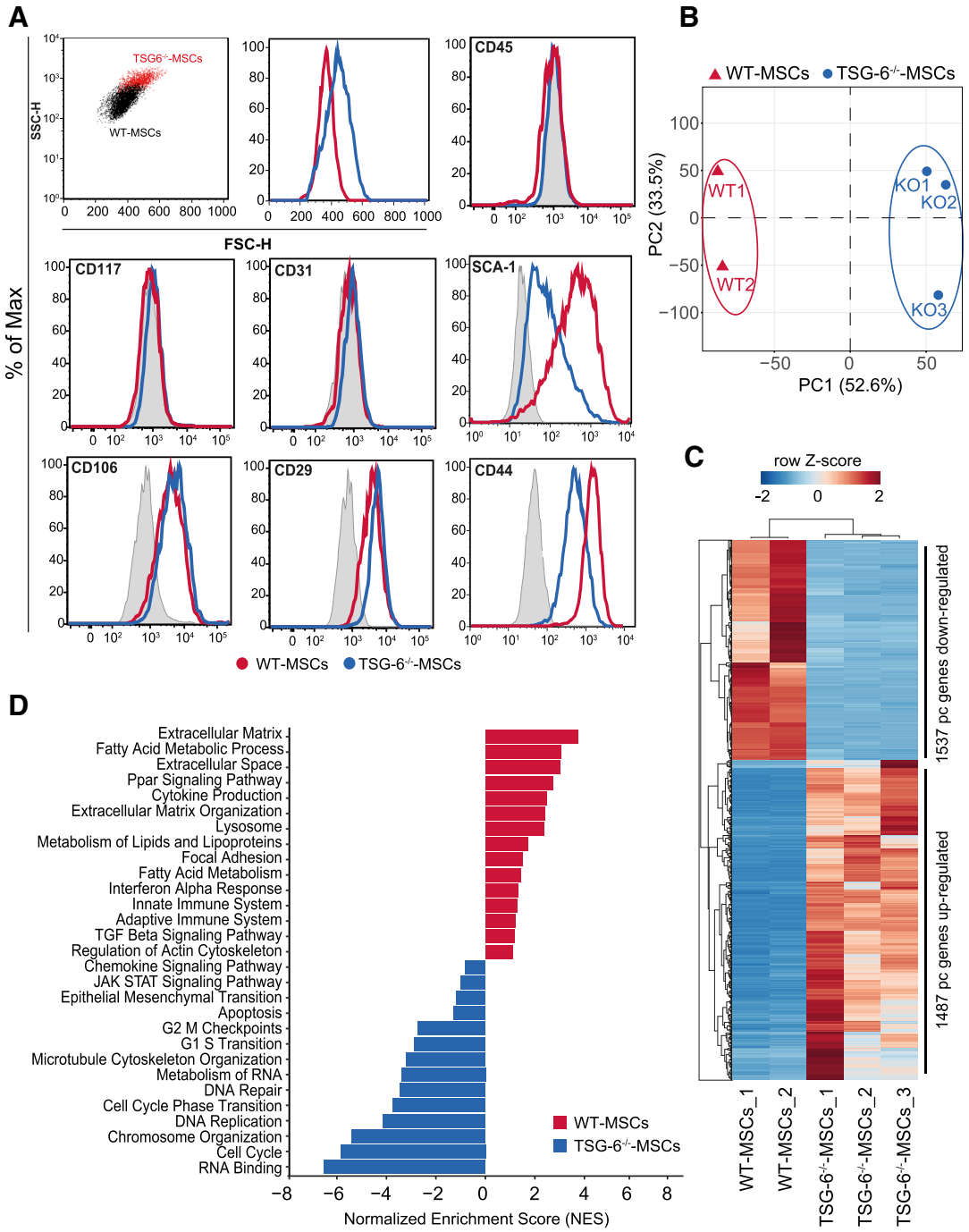

Figure 1. Characterization of wild-type (WT) and TNF-stimulated gene (TSG)-6$^{-/-}$ murine mesenchymal stem cells (MSCs). **(A):** Dot plot of size scatter height versus forward scatter (FSC) flow cytometric analysis of hematopoietic (CD45, CD117), endothelial (CD31), and stemness markers (SCA-1, CD106, CD29, CD44) performed on three different clones of WT-MSCs (red line) and TSG-6$^{-/-}$-MSCs (blue line) at passage 7. Control cells are shown as solid gray histograms. The data are expressed as %max; scaling is achieved by normalizing to 100% peak height at mode of distribution. **(B):** Principal component analysis plot showing distinct distribution of samples. WT-MSCs and TSG-6$^{-/-}$-MSCs are segregated into separate groups across the PC1 axis. **(C):** Hierarchical clustering of protein coding transcripts differentially expressed between WT-MSCs and TSG-6$^{-/-}$-MSCs (FDR < 0.1) showing 1,487 genes upregulated and 1,537 genes downregulated in TSG-6$^{-/-}$-MSCs compared with WT-MSCs. **(D):** Gene set enrichment analysis of biological processes and canonical pathways for differentially expressed genes categorized based on normalized enrichment score. WT-MSCs (red, n = 2) and TSG-6$^{-/-}$-MSCs (blue, n = 3). Abbreviation: PC, principal component.

were also characterized by larger cytoplasm and nucleus volume (p < .0001; Fig. 2D). These morphological differences were consistent with the different SSC-H and FSC values between the two groups of cells (Fig. 1A), thus reflecting distinct physical properties of TSG-6$^{-/-}$-MSCs and WT-MSCs. The morphological analysis of the cytoskeleton organization performed on the Z-projection of the F-actin confirmed a dissimilar distribution and expression of actin between TSG-6$^{-/-}$-MSCs and WT-MSCs.

Whilst WT-MSCs showed abundant actin filaments particularly surrounding the nuclei and beneath the plasma membrane, TSG-6$^{-/-}$-MSCs displayed more diffuse and weaker actin staining in these locations (Fig. 2E). Although larger than WT cells, TSG-6$^{-/-}$-MSCs cells had almost twofold lower actin levels (shown as integrated density in Fig. 2F; $p = .0004$), with lower aspect *ratio* and higher circularity (Fig. 2G). These data confirmed cytoskeletal arrangements with a shift toward rounded cell morphology in TSG-6$^{-/-}$-MSCs. In addition to actin changes, decreased expression of dynamin 1 in TSG-6$^{-/-}$-MSCs (Supporting Information Fig. S1B), a GTPase protein encoded by Dnm1 that along with actin plays a role in the formation of vesicles originating from the plasma membrane [32], raised the possibility of a defect in the release of extracellular vesicles that are accountable for MSC-trophic effects [33] in TSG-6-deficient cells. To address this point, we quantified the production of exosomes (EXs) and microvesicles (MVs) in the supernatant of MSCs. No differences were found between WT-MSCs and TSG-6$^{-/-}$-MSCs in terms of total protein concentration, as assessed using the Bradford assay (MVs: 37.8 μg in TSG-6$^{-/-}$-MSCs and 34.65 μg in WT-MSCs; EXs: 11.25 μg in TSG-6$^{-/-}$-MSCs and 8.6 μg in WT-MSCs), and the number of extracellular vesicles, as measured using dynamic light scattering. However, TSG-6$^{-/-}$-MSCs generated significantly smaller EXs and MVs in comparison to WT-MSCs (Fig. 2H; $p < .05$, $p < .01$). Altogether, these results strongly indicate that TSG-6 plays an important role in several biological processes dependent on actin cytoskeleton organization in MSCs.

TSG-6$^{-/-}$-MSCs Display Proliferative and Expansion Defects

IPA analysis on TSG-6$^{-/-}$ and WT-MSCs identified a significant modulation in the expression of genes involved in the cell cycle. These data were further confirmed by GSEA analysis performed on the cell cycle gene set, showing a significant negative enrichment of genes regulating processes that stop, prevent, or reduce frequency, rate, extent, and direction of the cell cycle (Fig. 2I). To validate this finding, we next analyzed the cell cycle distribution of the two cell lines after serum deprivation. After 24 hours of incubation in serum-free medium, cells lacking TSG-6 arrested at the G_0/G_1 phase of the cell cycle with a significant reduction of S-phase as compared with WT-MSCs (Fig. 2J). Moreover, TSG-6$^{-/-}$-MSCs displayed reduced clonogenic potential (Fig. 2K), which is a distinct feature of MSCs [34] and cell proliferation (i.e., as assessed at 24 and 48 hours of culture) compared with WT-MSCs (Fig. 2L).

TSG-6 Deficiency Causes Loss of the Multilineage Differentiation Potential of MSCs

High proliferation potential, clonal expansion capacity, and ability to differentiate into mesenchymal lineages are all regarded as distinctive stem cell characteristics of MSCs [1]. The finding that loss of TSG-6 impacted on the proliferative and clonal expansion capacities of MSCs prompted us to evaluate whether genetic depletion of this gene also affected the multilineage differentiation potential of MSCs. We found that TSG-6$^{-/-}$-MSCs were unable to differentiate into adipocytes after 14 days of culturing in adipogenic conditioned medium, as opposed to WT-MSCs, which differentiated into Oil Red O-positive adipocytes (Fig. 3A). However, addition of recombinant murine TSG-6 (rmTSG-6; 5 ng/ml) to the conditioned medium rescued the adipogenic potential of TSG-6$^{-/-}$-MSCs, indicating that TSG-6 expression is required for the differentiation of MSCs to adipocytes. Indeed, TSG-6 mRNA levels significantly increased in WT-MSCs over the 14-days of adipogenic differentiation (Fig. 3B). Since GSEA analysis revealed a significant downregulation of genes involved in the regulation of adipogenic differentiation (Fig. 3C), we analyzed the expression of two critical transcription factors (TFs) for this process, the early B cell factor (EBF-1) and the peroxisome proliferation-activated receptor-γ 2 (PPAR-γ2) [35]. Both TFs were upregulated in WT-MSCs, but not in TSG-6$^{-/-}$-MSCs during adipogenic differentiation (Fig. 3D). Interestingly, administration of exogenous rmTSG-6 restored PPAR-γ2 and EBF-1 expression in TSG-6$^{-/-}$-MSCs (Fig. 3D), thus supporting the hypothesis that TSG-6 acts as a key regulator of the mesenchymal adipogenic differentiation.

Based on these findings, we explored whether loss of TSG-6 impacted also on the ability of MSCs to differentiate into other cell types such as osteoclasts and chondrocytes. TSG-6$^{-/-}$-MSCs failed to differentiate into osteogenic cells (Fig. 3E). Expression of two major TFs involved in osteogenic differentiation, Runt related transcription factor 2 (Runx2) and transcription factor Sp7 (Osterix) [35] did not change in TSG-6$^{-/-}$-MSCs over the 14-days of osteogenic differentiation. By contrast, both TFs were highly upregulated in differentiated WT-MSCs (Fig. 3F). However, addition of rmTSG-6 was not sufficient to rescue osteogenic differentiation and Runx2 and Osterix induction in TSG-6$^{-/-}$-MSCs (Fig. 3F). Similar results were observed when the chondrogenic differentiation potential of these cells was assessed. Indeed, WT-MSCs reacted with the Alcian blue dye, which stains extracellular components of the cartilage matrix (e.g., proteoglycans), whereas TSG-6$^{-/-}$-MSCs did not (Fig. 3G). GSEA analysis on the chondrocyte differentiation gene set identified 24 genes that were significantly modulated in TSG-6$^{-/-}$-MSCs compared with WT-MSCs (Fig. 3H). Among these genes, SRY-Box 9 (Sox-9) and bone morphogenetic protein 2 (Bmp2), two crucial factors for condensation and differentiation to chondrocytes, were downregulated in the absence of TSG-6. Altogether, these results demonstrate that TSG-6 regulates the differentiation capacities of MSCs.

Protein Enrichment of the ECM Rescues Cell Morphology and Proliferation in TSG-6$^{-/-}$-MSCs

TSG-6 is involved in the organization and stabilization of the ECM interacting with glycosaminoglycans such as HA and heparan sulfate [18, 36, 37]. In line with this, GSEA analysis showed enrichment of the *"extracellular space"* gene set in WT-MSCs compared with TSG-6$^{-/-}$-MSCs (Fig. 4A). In the absence of TSG-6, the genes involved in the ECM-cell interactome, including the cell division control protein 42 homolog (Cdc42) that is known to play a key role in actin remodeling, were downregulated (Supporting Information Fig. S2A, S2B). Given that ECM-interactions either directly or indirectly control fundamental cellular processes such as adhesion, migration, and proliferation [38], we explored whether the loss of TSG-6-mediated changes in the extracellular environment can affect some of these cellular functions. To address this point, TSG-6$^{-/-}$-MSCs were plated for 48 hours at 37°C on top of a HA-based scaffold, in the absence (nonsupplemented) or in the presence (supplemented) of TSG-6 and other ECM proteins, such as pentraxin-3 (PTX3), which is known to cooperate with TSG-6 in the assembly and organization of HA matrices [20, 39]. We then analyzed cell morphology and proliferation (Fig. 4B). When cultured on the supplemented scaffold, TSG-6$^{-/-}$-MSCs appeared

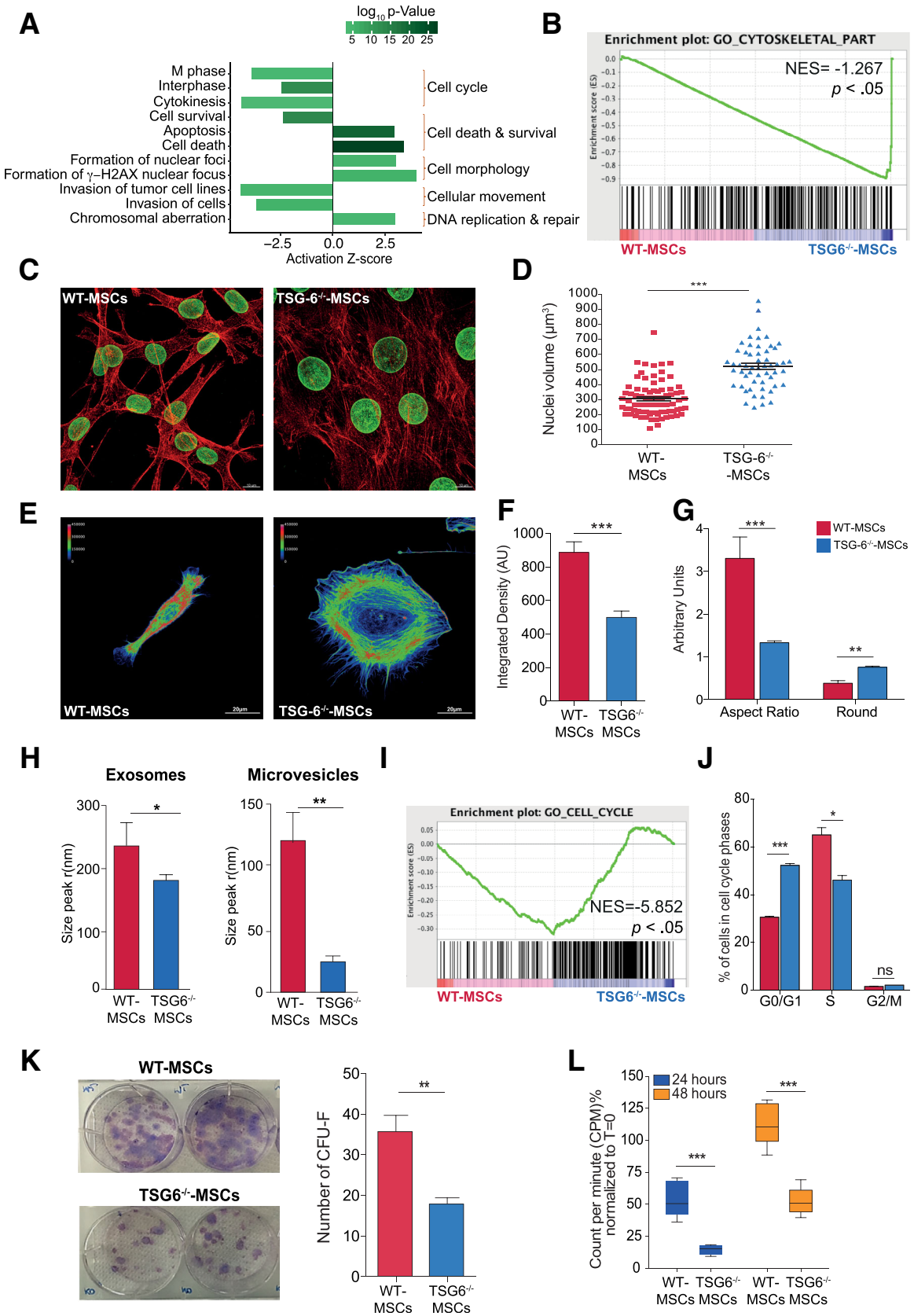

Figure 2. The loss of TNF-stimulated gene (TSG)-6 impacts the phenotype of mesenchymal stem cells (MSCs) in terms of morphology and proliferation features. **(A):** Top canonical pathways identified by Ingenuity Pathway Analysis and categorized based on their *Z*-score algorithm in three clones of TSG-6$^{-/-}$-MSCs compared with two clones of wild-type (WT)-MSCs. Bar color threshold indicates significant

(Figure legend continues on next page.)

as elongated and crescent-shaped cells (Fig. 4C) showing a morphology similar to WT-MSCs (Supporting Information Fig. S3A), although they maintained larger nuclear size than WT-cells (Supporting Information Fig. S3B). However, in comparison to TSG-$6^{-/-}$-MSCs cultured directly on plastic or on nonsupplemented scaffold they displayed smaller nuclei ($p < .05$ and $p < .0001$, respectively; Fig. 4D). In addition, on the HA scaffold TSG-$6^{-/-}$-MSCs significantly increased their proliferative rate ($p = .0121$). This effect was more enhanced after supplementation of the scaffold (Fig. 4E). These observations support a key role for ECM components and in particular for TSG-6 in modulating cell morphology and proliferation of MSCs.

Loss of TSG-6 Alters Several Transcription Factors Crucial for Stem Cell Properties

Morphological, proliferative, and differentiation changes observed in MSCs upon TSG-6 depletion could be due to alterations in regulatory pathways, as suggested by upstream analysis in IPA (Fig. 4F). In particular, TSG-$6^{-/-}$-MSCs had more inhibited genes than activated genes compared with WT-MSCs ($p < .01$), especially with reference to those coding for transcription regulators (44 versus 26, respectively), growth factors (9 versus 1), enzymes (28 versus 20), and cytokines (11 versus 5; Fig. 4F). Loss of TSG-6 led to perturbation of the expression of TFs, perhaps supporting TSG-6 as an extrinsic regulator of TFs (Fig. 5A). Notably, gene ontology analysis (performed on the differentially expressed genes; i.e., with fold changes of ≥2 or ≤−2) revealed that the expression of several TFs targeting genes involved in the regulation of cell division, stem cell differentiation, mesenchymal differentiation, and the Wnt signaling pathway (Fig. 5B, Supporting Information Fig. S4) were inhibited upon TSG-6 depletion. Thereby, these data provide corroborating evidence that TSG-6 is a regulator of several biological properties of MSCs.

Activated TSG-$6^{-/-}$-MSCs Are More Prone to Release IL-6 Than WT-MSCs

The anti-inflammatory properties of MSCs are taken as a cornerstone of MSC-based therapies. Previously, we reported a defective release of anti-inflammatory cytokines in TSG-6 deficient MSCs (i.e., IL-10) with an unbalanced production of pro-inflammatory cytokines (i.e., IL-17, interferon γ, TNF-α) [30]. Here, IPA analysis identified a global perturbation in the expression of cytokine genes upon TSG-6 depletion. Since in vivo implantation of MSCs increased levels of pro-inflammatory cytokine IL-6 compared with WT-MSCs [30], we assessed whether TSG-6 could modulate the production of IL-6. To this end, we measured the levels of IL-6 in the culture supernatant of TSG-$6^{-/-}$-MSCs and WT-MSCs. Both MSC cultures had comparable amount of IL-6 (TSG-$6^{-/-}$-MSCs: 917 ± 56; WT-MSCs: 760 ± 113 pg/total number cells per well; Fig. 6A). Since activated (AT) immune cells induce MSCs to produce IL-6 [40], we cocultured both groups of MSCs in the presence of non-AT or AT splenocytes. As expected, the levels of IL-6 markedly increased in the coculture of MSCs with AT splenocytes (SPLC; Fig. 6A). To determine whether the cytokine was produced by MSCs, we plated MSCs at different ratios with SPLC (1:2.5; 1:5; 1:20) and after 24 hours, we collected the supernatants for the measurement of IL-6. The IL-6 concentration markedly increased when AT SPLC were present at 2.5-fold or 5.0-fold higher levels than MSCs (MSCs:SPLC 1:2.5 and 1:5 ratios) but decreased when the *ratio* was 1:20. Non-AT and AT SPLC displayed significantly lower IL-6 secretion in comparison of MSCs (Fig. 6A). The normalization of IL-6 levels based on the number of MSCs per well showed a linear correlation between number of MSCs and IL-6 concentration (Fig. 6B). The analysis of IL-6 mRNA from recovered MSCs correlated with the protein data. MSCs at a ratio 1:2.5 to immune cells displayed higher expression of IL-6 mRNA compared with those at a ratio of 1:5 and to MSCs alone (Supporting Information Fig. S5). These data confirm that MSCs upregulate their secretion of IL-6 in the presence of AT immune cells. Notably, TSG-$6^{-/-}$-MSCs at all ratios exhibited substantially greater release of IL-6 compared with WT cells ($p < .05$; Fig. 6A, 6B and Supporting Information Fig. S5) supporting a role of TSG-6 in the regulation of IL-6 production in MSCs.

TSG-$6^{-/-}$-MSCs Conditions the Tumor Microenvironment

IL-6 is a key mediator of the inflammatory response [41] and has a pathological role in the development of several tumors [42, 43]. Indeed, high serum concentrations of IL-6 have been reported to correlate with a poor outcome in cancer patients including colorectal, melanoma, and lung cancer [44, 45]. Recent

(Figure legend continued from previous page.)
p-value reported in logarithmic scale to base 10. **(B):** Gene set enrichment analysis (GSEA) showing significant negative enrichment of "*cytoskeletal part*" gene set in TSG-$6^{-/-}$-MSCs with respect to WT-MSCs (normalized enrichment score [NES] = −1.267; $p < .05$). **(C):** Representative immunofluorescence images showing costaining of F-actin (red) and Lamin B1 (green) in WT-MSCs (*left panel*) and TSG-$6^{-/-}$-MSCs (*right panel*) after 48 hours of culture. White scale bar: 10 μm. **(D):** Nuclei volumes of WT-MSCs and TSG-$6^{-/-}$-MSCs expressed in μm^3 as calculated by Imaris software (Bitplane). **(E):** Representative confocal images of isolated WT-MSCs and TSG-$6^{-/-}$-MSCs. Colors correspond to the F-actin expression as indicated by the color scale (white scale bar: 20 μm). **(F):** Graph showing integrated density of F-actin and **(G)** cell shape descriptors of the actin-cytoskeleton in WT-MSCs and TSG-$6^{-/-}$-MSCs quantified using ImageJ software suite and reported in arbitrary units. **(H):** Size distribution analysis of purified exosomes (*left panel*) and microvesicles (*right panel*) assessed by dynamic light scattering and expressed as size peak radius (nm) indicate the distribution of values for WT (red) and TSG-$6^{-/-}$ (blue) MSCs ($n = 3$). **(I):** GSEA showing significant negative enrichment of "*cell cycle*" gene set in TSG-$6^{-/-}$-MSCs with respect to WT-MSCs (NES = −5.852; $p < .05$). **(J):** Cell cycle of WT-MSCs and/or TSG-$6^{-/-}$-MSCs analyzed by flow cytometry analysis after 48 hours of seeding. Cells were gated based on forward and side scatter to separate debris, and then the cellular events were further gated based on their BrdU and 7-AAD content. Results are expressed as percentage of the cells gated in the various cell cycle phases ($n = 2$). **(K):** Colony-forming unit assay. (*Left panel*) Formed colonies visualized with Giemsa staining after 14 days for WT-MSCs (on the top) and TSG-$6^{-/-}$-MSCs (on the bottom); (*right panel*) bar graph showing the number of colony forming cells from WT-MSCs and TSG-$6^{-/-}$-MSCs. **(L):** Time course over 48 hours of the proliferation rate of WT-MSCs and/or TSG-$6^{-/-}$-MSCs incorporating [^{3}H]-thymidine. Results are expressed as a percentage of cell proliferation normalized on time zero ($n = 4$ independent experiments); *, $p < .05$; **, $p < .01$; ***, $p < .001$ by *t* test; or by analysis of variance.

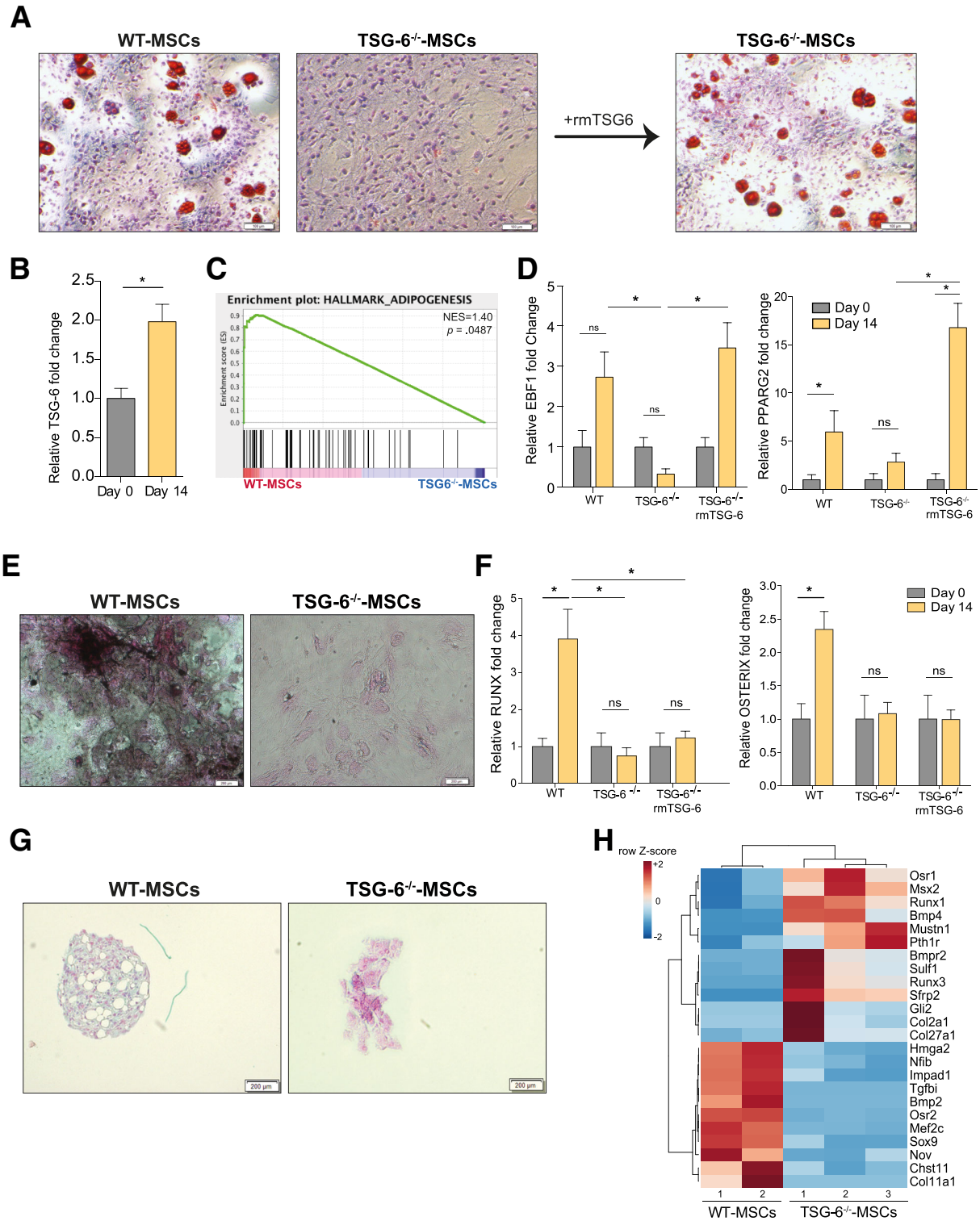

Figure 3. Mesenchymal stem cells (MSCs) lacking TNF-stimulated gene (TSG)-6 lose their differentiation capability. **(A):** Representative pictures of adipogenic differentiation of wild-type (WT)-MSCs and TSG-6$^{-/-}$-MSCs. Accumulated lipid vacuoles were detected by Oil Red O staining after 14 days of stimulation (lipid vacuoles in red) in absence or presence of recombinant murine TSG-6 (rmTSG-6, 5 ng/ml). Black scale bar: 100 μm. **(B):** qRT-polymerase chain reaction (PCR) quantification of TSG-6 expression in WT-MSCs at day-0 (gray bar) and at day-14 of adipogenic differentiation (yellow bar); *, $p < .05$ by t test. **(C):** Gene set enrichment analysis identified positive enrichment of WT-MSCs in "*adipogenesis hallmark*" gene set (normalized enrichment score [NES] = 1.40; $p = .0487$). **(D):** qRT-PCR quantitation of EBF-1 and PPARγ2 gene expression in WT-MSCs, TSG-6$^{-/-}$-MSCs alone and/or in presence of rmTSG-6 (5 ng/ml) at day-0 (gray bars) and at day-14 of adipogenic differentiation (yellow bars). **(E):** Representative pictures of osteogenic differentiation of WT-MSCs and TSG-6$^{-/-}$-MSCs. Deposited calcified matrix was visualized by Von Kossa staining at day-14 (calcified matrix in black; black scale bar: 200 μm).

(Figure legend continues on next page.)

studies have shown that human bone marrow-derived MSCs can enhance cancer cell proliferation via the IL-6 signaling pathway [46, 47]. Given the high levels of IL-6 produced in TSG-6$^{-/-}$-MSCs, it was of interest to determine whether the loss of TSG-6 could sustain pro-tumoral effects of MSCs. To investigate this possibility, we exploited the effect of MSCs on tumor development in a colitis-associated model of CRC in which IL-6 has profound impact on tumorigenesis [48, 49]. Interestingly, we observed that mice receiving allogeneic TSG-6$^{-/-}$-MSCs displayed a significant increased number of tumor lesions compared with either untreated (phosphate-buffered saline [PBS]) or WT-MSCs-treated groups, as determined by endoscopic and histological recordings (Fig. 6C, 6D). Of note, the incidence of tumors correlated with high serum levels of IL-6 (Fig. 6E). Indeed, mice treated with TSG-6$^{-/-}$-MSCs displayed higher levels of IL-6 than those receiving WT-MSCs cells; i.e., consistent with the loss of TSG-6 in MSCs enhancing the release of IL-6 (see above), which could have the effect of amplifying the pro-tumorigenic effects of MSCs in specific tissues.

MSCs have been shown to have tumor-promoting effects stimulating directly tumor growth [13, 50–54]. In order to explore whether the lack of TSG-6 exacerbates this effect, we evaluated tumor growth in xenograft models by subcutaneously implanting two different adenocarcinoma cell lines (A549 lung cancer cell line or colon cancer cell line Caco-2) in coadministration with MSCs (Fig. 6F). Here, none or small tumor lesions were observed after the injection of A549 and Caco-2 cells alone. In both models, coadministration of MSCs boosted tumor growth (Fig. 6G, 6H), thus confirming the capacity of MSCs to promote tumor cell growth [55]. Nevertheless, no statistically significant difference in tumor volume was found between mice receiving TSG-6$^{-/-}$-MSCs and WT-MSCs, thus excluding a defect in TSG-6 as a direct cause in promoting tumor growth.

Discussion

This study provides the first evidence of the important role played by TSG-6 in the definition of stemness and other biological properties of murine MSCs, conferring to these cells an anti-inflammatory phenotype and reducing their pro-tumorigenic effects. Thus, in addition to mediating the anti-inflammatory and reparative properties of MSCs by acting as a paracrine factor on different cell targets [18, 26–30], TSG-6 can also act as an autocrine factor regulating MSC cellular processes. An autocrine function has been reported previously for TSG-6 in regulating the bone resorbing properties of human osteoclasts [36].

Loss of TSG-6, in fact, not only affects the immunomodulatory capacities of MSCs as previously described [18], but also strongly influences quantity and organization of actin, cell morphology, proliferation, and cell differentiation. Actin filaments in active cells are highly concentrated at the periphery of the cell, where they form a three-dimensional network beneath the plasma membrane supporting mechanical properties, determining cell shape, and a variety of cell surface activities including division and migration.

Interestingly, in the absence of TSG-6, the actin filaments appeared to be localized mainly around nuclei with a discontinuity in close proximity to the plasma membrane, resulting in enlarged rounded cell shape characterized by large nuclei similar to senescent cells. Indeed, during cellular senescence, mesenchymal cells change their morphology from a spindle shape to an enlarged, flattened, and irregular shape, associated with enlarged and often irregular nuclei and chromatin reorganization that leads to a reduced cell proliferation [56]. Although TSG-6$^{-/-}$-MSCs displayed a reduced proliferative ability, with an arrest of cells into the G_0/G_1 phase of the cell cycle compared with WT cells, the transcriptome profile of these cells was not consistent with inactive and senescent cells. In support of this, the expression of nuclear lamin B1, which is considered a senescence-associated biomarker [57] did not differ between TSG-6$^{-/-}$-MSCs and WT-MSCs. TSG-6 exerts a large number of activities including the modulation of immune and stromal cell function, regulation of ovulation, inhibition of the protease network, and promotion of tissue regeneration [16–18]. The wide functional repertoire of TSG-6 reflects its ability to regulate matrix organization, to control the association of matrix molecules with cell surface receptors and extracellular signaling factors such as chemokines [18, 24, 25]. In particular, TSG-6 is able to interact with glycosaminoglycans such as HA and heparan sulfate [18], ubiquitous components of the ECM, for example, participating in the (re)organization of the newly formed ECM following inflammation and tissue injury [58]. By crosslinking HA, TSG-6 may drive reorganization of the HA receptors, such as LYVE-1 and CD44 on the cell surface and modulate their activity [21, 59]. TSG-6 is a potent modulator of HA binding to CD44 on lymphoid cell lines [21], which likely regulates leukocyte migration to the sites of inflammation. Interestingly, a recent study has demonstrated that the cell surface distribution of CD44 can restrict the movement of other receptors and influence the organization of the actin cytoskeleton [60, 61]. Our flow cytometry analyses revealed a reduction in the expression of CD44 on the surface of TSG-6$^{-/-}$-MSCs compared with WT cells. Therefore, the involvement of TSG-6 in actin organization and cellular morphology of MSCs could be due to its interaction with HA and heparan sulfate, that in turn impacts on cell shape and functional activities of MSCs through the stabilization of ECM components. Given the evidence for a role of heparan sulfate proteoglycans in exosome formation [62], and the possibility that TSG-6 could affect heparan sulfate

(Figure legend continued from previous page.)
(F): qRT-PCR quantitation of RUNX and OSTERIX genes in WT-MSCs, TSG-6$^{-/-}$-MSCs alone and in presence of rmTSG-6 at day-0 (gray bars) and at day-14 of osteogenic differentiation (yellow bars). **(G):** Representative pictures of chondrogenic differentiation of WT-MSCs and TSG-6$^{-/-}$-MSCs. Cartilage glycosaminoglycans were visualized by Alcian Blue staining at day 21 (glycosaminoglycans in blue, cell nuclei in pink; black scale bar: 200 μm). **(H):** Hierarchical clustering of the gene set (24 genes) related to the chondrocyte differentiation differentially expressed between WT-MSCs and TSG-6$^{-/-}$-MSCs (FDR < 0.1). For all qRT-PCR results, data reflect mean ± SEM from four independent experiments, the results were normalized to glyceraldehyde-3-phosphate dehydrogenase (GAPDH) mRNA and to the condition "time zero," considered as 1. *, $p < .05$ by one-way analysis of variance ($n = 3$ independent experiments).

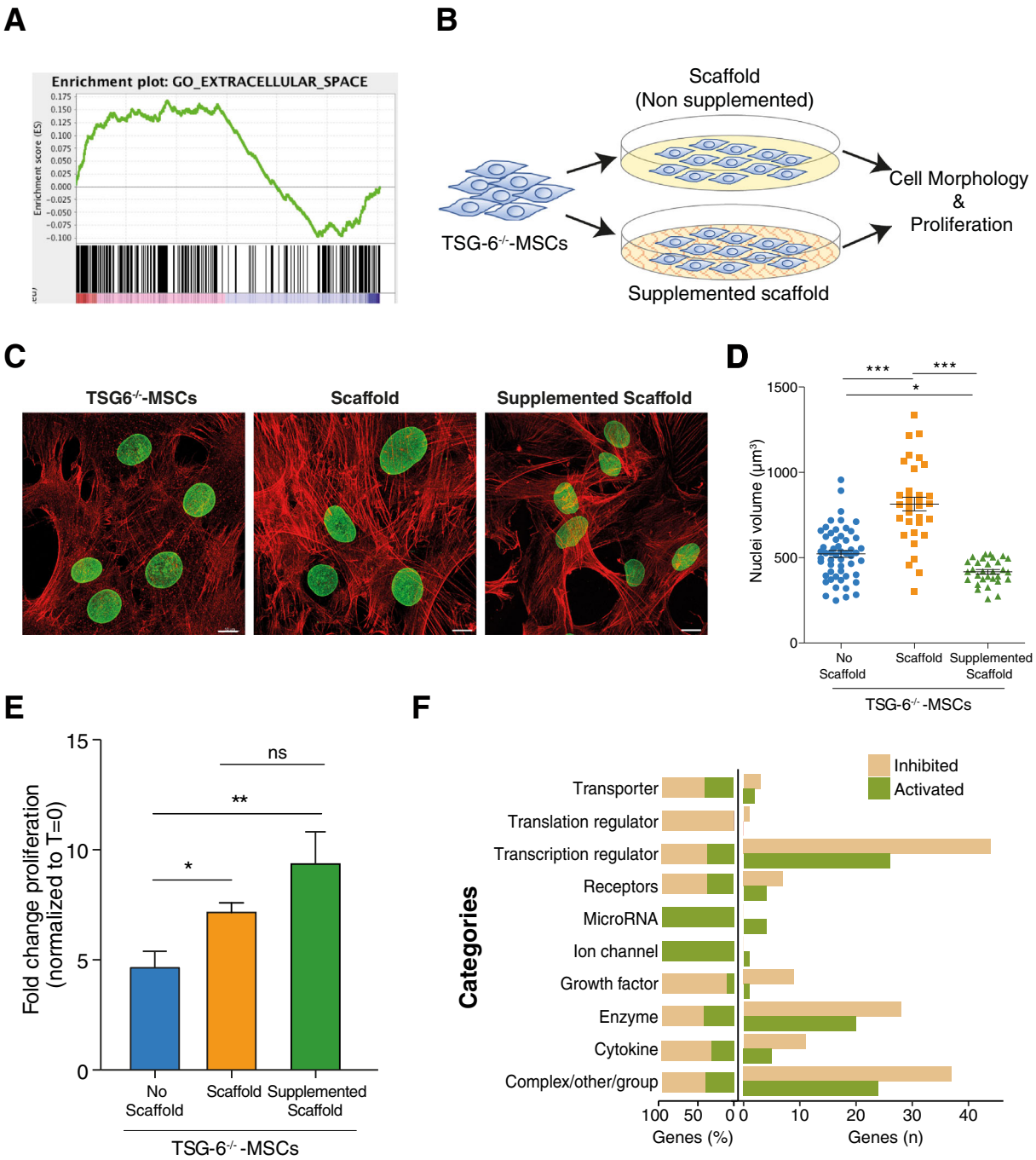

Figure 4. TNF-stimulated gene (TSG)-6 is a crucial factor for the stabilization of the extracellular matrix. **(A):** Gene set enrichment analysis positive enrichment plot of wild-type (WT)-mesenchymal stem cells (MSCs) in "*extracellular space*" gene set (normalized enrichment score [NES] = 3.017). Statistical significant enrichment (p = .002) of genes involved in extracellular space were higher in WT-MSCs compared with TSG-6$^{-/-}$-MSCs. **(B):** Illustration depicting the experimental workflow for the analysis of cellular morphology and proliferation of TSG-6$^{-/-}$-MSCs plated on top of a HA-based scaffold. The cells were seeded at the density of 20,000 cells per cm^2 for 48 hours in the absence (nonsupplemented scaffold) and presence (supplemented scaffold) of rmTSG-6 (0.15 µM), rmPTX3 (0.15 µM), and mouse serum (5%). **(C):** Representative confocal immunofluorescence images showing colocalization of F-actin (red) and Lamin B1 (green) in TSG-6$^{-/-}$-MSCs plated without scaffold (*left panel*), on the scaffold (TSG-6$^{-/-}$-MSCs + scaffold; *central panel*), and on the supplemented scaffold (TSG-6$^{-/-}$-MSCs + scaffold supplemented; *right panel*). White scale bar: 10 µm. **(D):** Nuclei volume expressed in µm^3 and calculated by Imaris software (Bitplane). **(E):** Proliferation rate of TSG-6$^{-/-}$-MSCs evaluated by using radiolabeled thymidine after 48 hours plated without scaffold (no scaffold), or on the scaffold without supplementation (scaffold), or on the supplemented scaffold. Results are representative of three independent experiments each characterized by six replicates and expressed as fold change of proliferation normalized on time zero. **(F):** Ingenuity Pathway Analysis upstream regulator analysis used to identify putative upstream regulators activated (green) or inhibited (orange) in three clones of TSG-6$^{-/-}$-MSCs compared with two clones of WT-MSCs. p-Value is calculated using Fisher's exact test. *, $p < .05$ and ***, $p < .001$ by one-way ANOVA followed by Bonferroni multiple comparisons test.

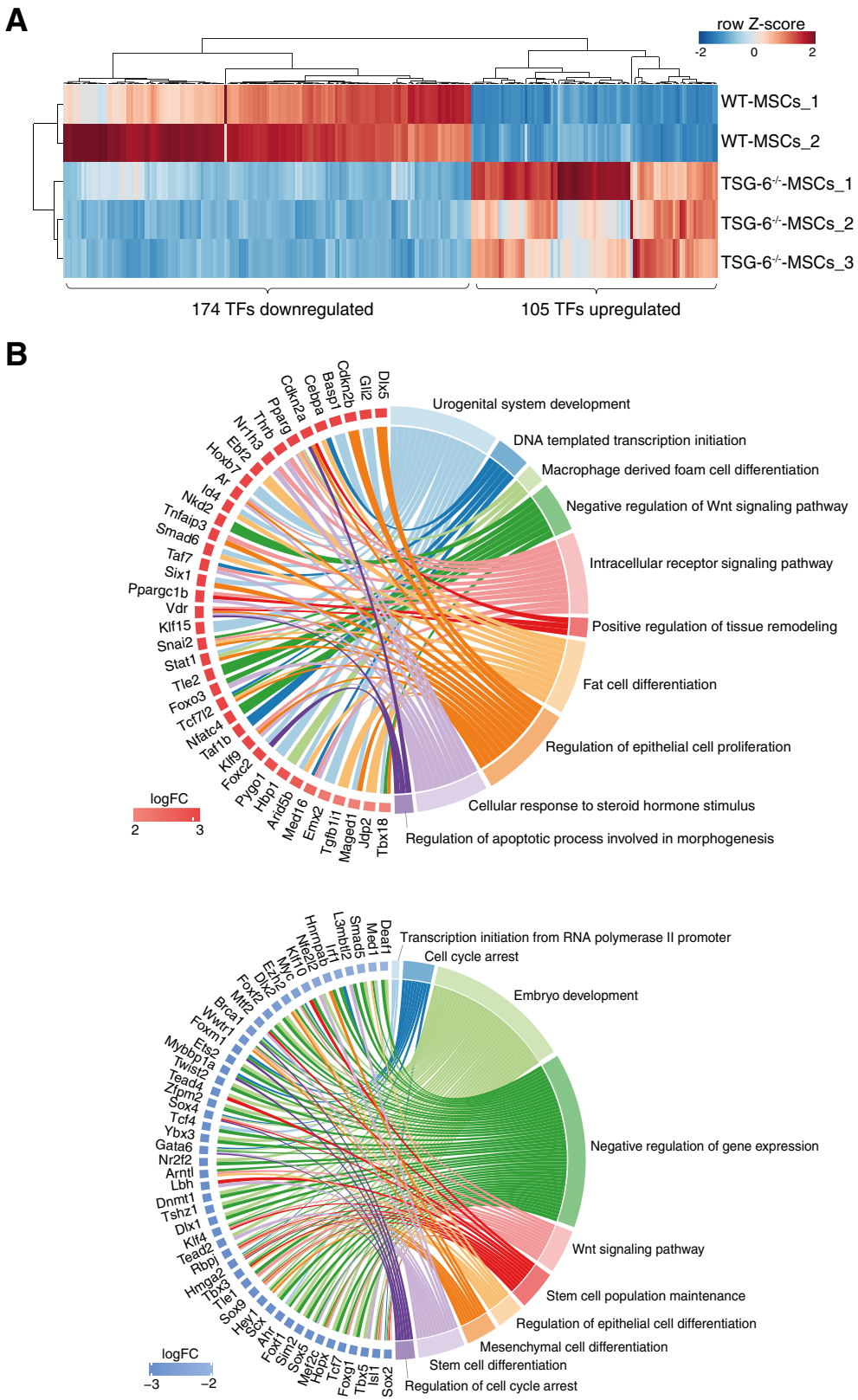

Figure 5. TNF-stimulated gene (TSG)-6 regulates the modulation of transcription factors. **(A):** Hierarchical clustering of 279 transcription factors (TFs) differentially expressed between two clones of wild-type (WT)-mesenchymal stem cells (MSCs) and three clones of TSG-6$^{-/-}$-MSCs (FDR < 0.1) showing 105 TFs upregulated and 174 TFs downregulated. **(B):** GO analysis of upregulated (*top panel*) and downregulated (*bottom panel*) TFs in TSG-6$^{-/-}$-MSCs. Circos plot visualization was performed using R package GOplot. Colored network connects each gene(s) with selected significantly enriched pathways (p < .05, Bonferroni correction) after semantic similarity. Genes present in at least two enriched GO were used for visualization of downregulated set.

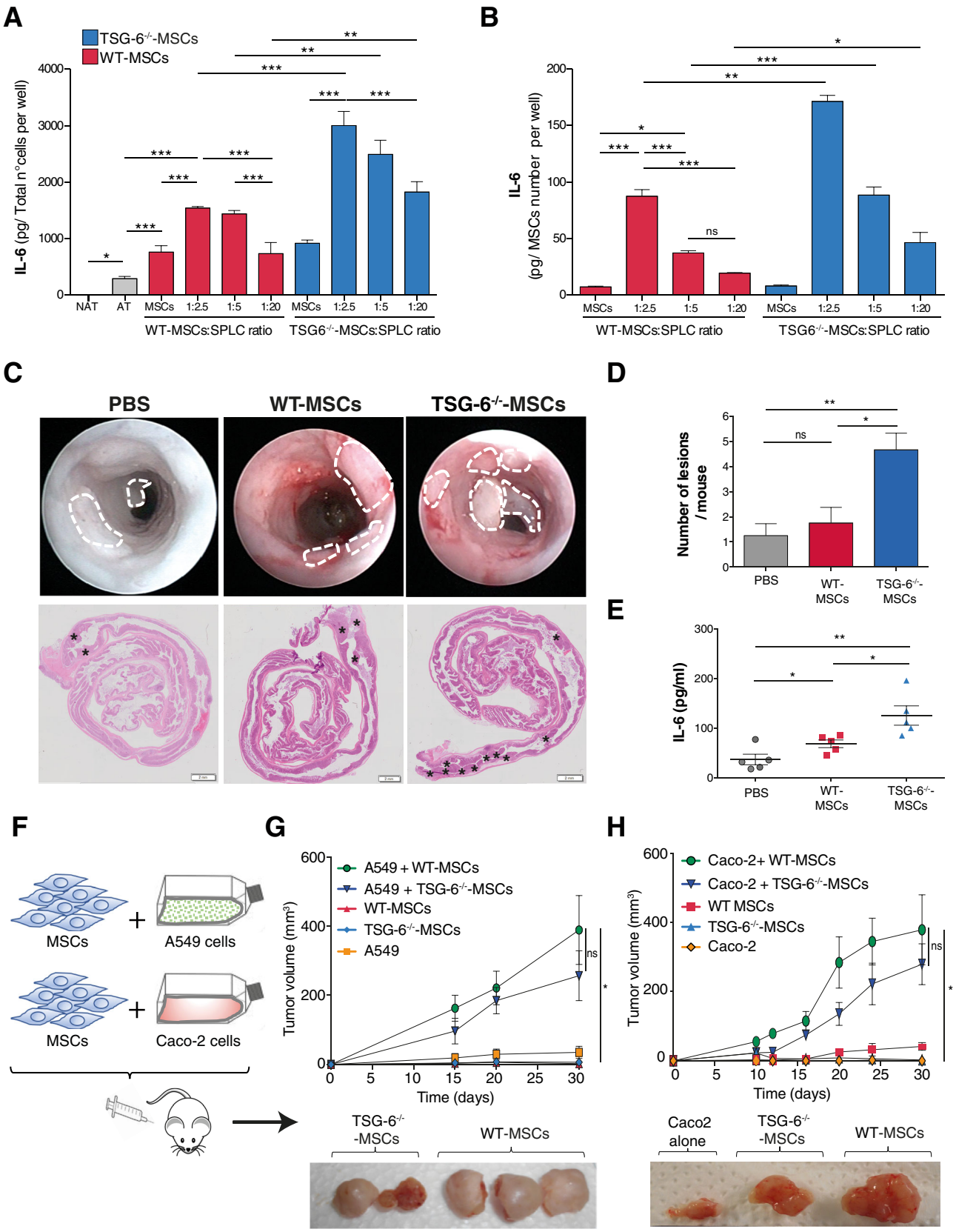

Figure 6. TNF-stimulated gene (TSG)-6 modulates interleukin (IL)-6 expression and affects tumor microenvironment. **(A, B):** IL-6 concentration determined by ELISA in the supernatants of nonactivated (NAT) or activated (AT) splenocytes (SPLC) alone or after 24 hours in coculture with MSCs at different ratios (MSCs: SPLC of 1:2.5, 1:5, and 1:20). *, $p < .05$; **, $p < .01$; ***, $p < .001$ by one-way analysis of

(Figure legend continues on next page.)

structure by crosslinking mechanisms [18], it is reasonable to suggest that TSG-6 influences extracellular vesicle formation through its interaction with ECM. However, the hypothesis that morphological and functional changes observed in TSG-$6^{-/-}$-MSCs are mediated by the loss of glycosaminoglycan—TSG-6 interaction, needs to be further investigated. Certainly, the deletion of TSG-6 leads to a decreased expression of gene products that interact with actin, such as dynamin1 that is involved in the formation of extracellular vesicles originating from the plasma membrane [32], and focal adhesion proteins including paxillin and Cdc42 that regulate the interaction of sites of cell adhesion to the ECM and actin polymerization [31, 63]. The ECM, consisting of a complex mixture of structural and functional macromolecules, serves an important role in cell organization and function such as adhesion, migration, proliferation, and differentiation. Improvements in cell morphology and proliferation (toward WT behavior) of TSG-6 deficient cells when cultured on a HA matrix scaffold supplemented with TSG-6 and PTX3 confirm a defective function of ECM in the absence of TSG-6. ECM provides the cells with important biomechanical cues that guide their behavior and fate through the activation of distinct transcriptional factors in MSCs [64, 65]. Failure of TSG-$6^{-/-}$-MSCs to differentiate into osteoblast and chondrocytes could be linked to changes in ECM. Both processes require specific transcriptional programs to be activated and/or repressed in a process of mechano-transduction from the ECM to the nucleus. Integrin-based focal adhesions with focal adhesion kinase are a mechano-sensitive signaling pathway that transmits signals from ECM to transcriptional machinery [66]. Interestingly, FAKs such as paxillin and Cdc42 are significantly downregulated in the transcriptome profile of TSG-$6^{-/-}$-MSCs. However, whether dysregulation of the ECM triggers all alterations observed in TSG-$6^{-/-}$-MSCs or whether there are additional mechanisms at play needs further investigations. Increased levels of TSG-6 found during preadipocyte differentiation [67] and the high TSG-6 expression in WT-MSCs fully differentiated to adipocytes identifies TSG-6 as a potential regulator of adipogenic differentiation. Indeed, here we discovered that MSCs deficient in TSG-6 failed to differentiate into adipocytes. Nevertheless, the addition of exogenous recombinant TSG-6 only rescued the MSC-adipogenic differentiation capacity and not MSC differentiation to chondrocytes or osteoblasts. These data raise two mechanisms of action on how TSG-6 regulates MSC biology, one as a modulator of the ECM, the other as an autocrine factor (that could be, at least in part, matrix-dependent). Overall, these results demonstrate that loss of TSG-6 triggers a cascade of changes in MSCs that affect differentiation processes and culminate in the abrogation of their stemness properties.

In 2006, the International Society of Cell Therapy (ISCT) identified minimal criteria for defining human multipotent MSCs, which were also extended to MSCs from animal origin. The criteria included their capacity to: adhere to plastic, give rise to colony-forming units, show positivity for specific stemness markers, and negativity for hematopoietic and endothelial markers and, finally, differentiate into three lineages (adipocytes, osteoblasts, and chondrocytes) [68]. Notably, although both WT and TSG-$6^{-/-}$-MSC lines adhered to plastic and were positive or negative for appropriate surface markers, TSG-$6^{-/-}$-MSCs fail to correspond to ISCT criteria in that they did not differentiate to adipocytes, osteoblasts, and chondrocytes. Although further studies are necessary to gain insight into the molecular mechanisms by which TSG-6 impacts differentiation processes, data from transcriptome profile analysis support TSG-6 as an extrinsic regulator of transcriptional factors essential to maintain stem cell properties. If confirmed in human MSCs, these findings could be relevant to the therapeutic use of MSCs, since they have become a very attractive cell source in regenerative medicine. TSG-6 may be used as a predictive marker of MSC effectiveness not only in terms of their immunomodulatory effects as already demonstrated [26–28], but also of their regenerative properties.

Loss of TSG-6 expression impacts on the anti-inflammatory properties of human and murine MSCs in vitro and in vivo in a wide range of disease models [18]. In the present study, IPA analysis identified a global perturbation in the expression of cytokine genes upon TSG-6 depletion confirming its role in the regulation of cytokines. With reference to this, we previously observed a failure of TSG-$6^{-/-}$-MSCs to improve intestinal inflammation [30]. In this study here, we explored whether TSG-6 could modulate the production of IL-6. Human and murine MSCs secrete IL-6 in response to activated immune cells by which they exert immunomodulatory effects [40]. Consistent with these results, both WT-MSCs and TSG-$6^{-/-}$-MSCs in presence of activated SPLC released IL-6. Interestingly, TSG-$6^{-/-}$-MSCs responded more strongly to the activation with an increased IL-6 production compared with WT cells identifying TSG-6 as a potential regulator of IL-6.

IL-6 signaling is generally considered a key mediator of the inflammatory response and also to play a direct role in promoting tumor progression [69]. Increased levels of IL-6 have been correlated with a poor outcome in cancer patients including colorectal, melanoma, and lung cancer [44, 45]. Previous studies have provided evidence that human bone marrow-derived MSCs could enhance cancer cell proliferation and tumor progression via the IL-6 signaling pathway and reduce the sensitivity of cancer cells to antitumor drugs

(Figure legend continued from previous page.)
variance (ANOVA) followed by Bonferroni multiple comparison test; $n = 3$ independent experiments. IL-6 levels were reported as pg/number of total cells per well or as pg/MSCs number per well. **(C):** Endoscopic and histological evaluation of tumor lesions in a model of colitis-associated cancer induced by one injection of azoxymethane and followed by three cycles of DSS (each of 6 days) in drinking water ad libitum. At day-3 of each cycle, mice received 3×10^6 of WT-MSCs or TSG-$6^{-/-}$-MSCs by intraperitoneally injection or phosphate-buffered saline (PBS) as negative control. The presence of tumors is highlighted by white dashed lines in the endoscopic images, and by black asterisks in the histological images ($n = 6$). **(D):** Number of tumor lesions per mouse in untreated (PBS), WT-MSC, or TSG-$6^{-/-}$-MSC treated mice; *, $p < .05$; **, $p < .01$ by one-way ANOVA. **(E):** IL-6 protein levels (pg/ml) determined by ELISA in the serum of untreated (PBS), WT-MSC, or TSG-$6^{-/-}$-MSC treated mice; *, $p < .05$ and **, $p < .01$ by one-way ANOVA. **(F):** Schematic illustration of tumor growth in xenograft models of cancer. Nude mice were injected subcutaneously with 3×10^6 A549 cells or Caco-2 cells alone or in combination with 3×10^6 of WT-MSCs or TSG-$6^{-/-}$-MSCs. **(G, H):** in vivo tumor growth measured as tumor volume (mm^3) over a 30-day period ($n = 5$) and representative macroscopic images of tumors at day 30; *, $p < .05$; **, $p < .01$; ***, $p < .001$ by one-way ANOVA followed by Bonferroni's test. Abbreviation: ns, not significant.

[70–73]. Interestingly, the level of IL-6 was markedly higher in the cancer tissue-derived MSCs in comparison to bone marrow-derived MSCs, suggesting that IL-6 may act as a key mediator of the tumor-promoting activity of the former cells [73]. It is likely that the higher level of IL-6 production in TSG-6$^{-/-}$-MSCs accentuates their pro-tumorigenic properties; the studies described here in an in vivo model of colon cancer, in which IL-6 has profound impact on tumor development, supported this theory. We observed a correlation between number of tumors and serum levels of IL-6 among the groups of mice receiving TSG-6$^{-/-}$-MSCs, WT-MSCs, and PBS. TSG-6$^{-/-}$-MSC-based treatment resulted in increased levels of IL-6 and a higher incidence of tumors compared with WT-MSCs or vehicle control. Further studies are now needed to gain insight into the mechanisms linking the loss of TSG-6 with increased levels of IL-6 and tumor development. The function of MSCs in tumor microenvironments are unclear due to contradictory results from different studies in different cancer types. There is increasing evidence that MSCs can exert stimulatory [12, 55, 74–76] or inhibitory [77–81] effects on tumor growth and invasion through their direct or indirect interaction with tumor cells. However, the mechanisms remain poorly defined. Comparable effects of the WT and TSG-6 failed-deficient MSCs in promoting tumor growth excluded IL-6 production and the loss of TSG-6 as a direct cause of enhanced tumorigenesis. Considering that MSCs enter wounds to facilitate tissue repair and that a tumor is considered a wound that never heals [82], it is likely that TSG-6 deficient MSCs contribute indirectly (e.g., IL-6) to tumor progression by sustaining the inflammatory process and tumor microenvironment.

Conclusion

Our data reveal a fundamental role for TSG-6 in regulating the biological properties of murine MSCs. In addition to working as a paracrine factor on different cell targets exerting potent anti-inflammatory effects, TSG-6 can also act as an autocrine factor regulating the morphology and several key cellular processes in MSCs. The loss of TSG-6 triggers a cascade of changes in MSCs that affect differentiation processes and culminate in the abrogation of their stemness properties. These data, if confirmed in human MSCs, support a potential application of TSG-6 as a predictor of the efficacy of MSCs in terms of their immunomodulatory and regenerative effects. In this scenario, TSG-6 may represent a clinically useful marker of antitumorigenic risk and a predictive tool for monitoring the effectiveness of immunomodulatory and regenerative therapies. Future studies are needed to address the link between IL-6 and TSG-6 and to understand the increased ability of TSG-6$^{-/-}$-MSCs in promoting tumorigenesis.

Acknowledgments

This paper is dedicated to the loving memory of Dr. Roberta Romano. We thank V. Garlatti and C. Correale for cell culture technical support. This research was supported by grant Ministero della Salute (GR-2009 Convenzione 76) to S.V.; Fondazione Cariplo per la Ricerca under grant 2012/0678 to S.V.; My First AIRC Grant (MFAG) 2015 under grant 17795 to S.V.; "Fondazione Umberto Veronesi Grant 2016 postdoctoral fellowship" to B.R.; Young Investigator Grant from Ministero della Salute (GR-2011-02349539) to A.I.; and European Crohn's and Colitis Organization Fellowship 2018 to S.E. A.J.D. thanks "Versus Arthritis" for their long-term funding of his research into TSG-6.

Author Contributions

B.R.: conducted experiments, collected and analyzed data, contributed to the writing of the paper, final approval of manuscript; S.E.: conducted experiments, collected, analyzed and interpreted gene expression data and analysis, final approval of manuscript; M.E.: acquired and analyzed confocal images, final approval of manuscript; E.S.: isolated and cultured MSCs, final approval of manuscript; L.P.: performed in vivo experiments, final approval of manuscript; P.K., S.S., L.M.: analyzed RNA-sequencing data, final approval of manuscript; S.R.: performed WB assay, final approval of manuscript; D.L.: performed dynamic light scattering analysis, final approval of manuscript; A.A., F.S.C.: analyzed FACS data, final approval of manuscript; M.S., A.I.: contributed to set cell culture on scaffold, final approval of manuscript; V.A. analyzed histology, final approval of manuscript; S.D., F.U., A.A.I., A.S.: edited the paper, final approval of manuscript; A.J.D.: contributed to the writing of the paper, final approval of manuscript; S.V.: conceived and designed experiments, provided financial support and study materials, analyzed and interpreted data and wrote the paper, final approval of manuscript.

Disclosure of Potential Conflicts of Interest

A.J.D. declared stock ownership in Bessor Pharma from a previous role as a consultant. The other authors indicated no potential conflicts of interest.

Data Availability Statement

The data that support the findings of this study are available on request from the corresponding author, and relevant data are provided in the Supporting Information files.

References

1 Pittenger MF, Mackay AM, Beck SC et al. Multilineage potential of adult human mesenchymal stem cells. Science 1999;284:143–147.
2 Mosna F, Sensebe L, Krampera M. Human bone marrow and adipose tissue mesenchymal stem cells: A user's guide. Stem Cells Dev 2010;19:1449–1470.
3 Bartholomew A, Sturgeon C, Siatskas M et al. Mesenchymal stem cells suppress lymphocyte proliferation in vitro and prolong skin graft survival in vivo. Exp Hematol 2002;30:42–48.
4 Klyushnenkova E, Mosca JD, Zernetkina V et al. T cell responses to allogeneic human mesenchymal stem cells: Immunogenicity, tolerance, and suppression. J Biomed Sci 2005; 12:47–57.
5 Zappia E, Casazza S, Pedemonte E et al. Mesenchymal stem cells ameliorate experimental autoimmune encephalomyelitis inducing T-cell anergy. Blood 2005;106:1755–1761.
6 Corcione A, Benvenuto F, Ferretti E et al. Human mesenchymal stem cells modulate B-cell functions. Blood 2006;107:367–372.
7 Le Blanc K, Mougiakakos D. Multipotent mesenchymal stromal cells and the innate

immune system. Nat Rev Immunol 2012;12: 383–396.
8 Phinney DG. Functional heterogeneity of mesenchymal stem cells: Implications for cell therapy. J Cell Biochem 2012;113:2806–2812.
9 Yim H, Jeong H, Cho Y et al. Safety of mesenchymal stem cell therapy: A systematic review and meta-analysis. Cytotherapy 2016; 18:S132.
10 Bateman ME, Strong AL, Gimble JM et al. Concise review: Using fat to fight disease: A systematic review of nonhomologous adipose-derived stromal/stem cell therapies. Stem Cells 2018;36:1311–1328.
11 Ame-Thomas P, Maby-El Hajjami H, Monvoisin C et al. Human mesenchymal stem cells isolated from bone marrow and lymphoid organs support tumor B-cell growth: Role of stromal cells in follicular lymphoma pathogenesis. Blood 2007;109:693–702.
12 Karnoub AE, Dash AB, Vo AP et al. Mesenchymal stem cells within tumour stroma promote breast cancer metastasis. Nature 2007;449:557–563.
13 Zhu W, Xu W, Jiang R et al. Mesenchymal stem cells derived from bone marrow favor tumor cell growth in vivo. Exp Mol Pathol 2006;80:267–274.
14 Romieu-Mourez R, Coutu DL, Galipeau J. The immune plasticity of mesenchymal stromal cells from mice and men: Concordances and discrepancies. Front Biosci 2012;4:824–837.
15 Ren GW, Su JJ, Zhang LY et al. Species variation in the mechanisms of mesenchymal stem cell-mediated immunosuppression. Stem Cells 2009;27:1954–1962.
16 Milner CM, Day AJ. TSG-6: A multifunctional protein associated with inflammation. J Cell Sci 2003;116:1863–1873.
17 Wisniewski HG, Vilcek J. Cytokine-induced gene expression at the crossroads of innate immunity, inflammation and fertility: TSG-6 and PTX3/TSG-14. Cytokine Growth Factor Rev 2004;15:129–146.
18 Day AJ, Milner CM. TSG-6: A multifunctional protein with anti-inflammatory and tissue-protective properties. Matrix Biol 2018.
19 Baranova NS, Nileback E, Haller FM et al. The inflammation-associated protein TSG-6 cross-links hyaluronan via hyaluronan-induced TSG-6 oligomers. J Biol Chem 2011;286:25675–25686.
20 Baranova NS, Inforzato A, Briggs DC et al. Incorporation of pentraxin 3 into hyaluronan matrices is tightly regulated and promotes matrix cross-linking. J Biol Chem 2014;289: 30481–30498.
21 Lesley J, Gal I, Mahoney DJ et al. TSG-6 modulates the interaction between hyaluronan and cell surface CD44. J Biol Chem 2004;279: 25745–25754.
22 Baranova NS, Foulcer SJ, Briggs DC et al. Inter-alpha-inhibitor impairs TSG-6-induced hyaluronan cross-linking. J Biol Chem 2013; 288:29642–29653.
23 Kota DJ, Wiggins LL, Yoon N et al. TSG-6 produced by hMSCs delays the onset of autoimmune diabetes by suppressing Th1 development and enhancing tolerogenicity. Diabetes 2013;62:2048–2058.
24 Dyer DP, Thomson JM, Hermant A et al. TSG-6 inhibits neutrophil migration via direct interaction with the chemokine CXCL8. J Immunol 2014;192:2177–2185.
25 Dyer DP, Salanga CL, Johns SC et al. The anti-inflammatory protein TSG-6 regulates chemokine function by inhibiting chemokine/glycosaminoglycan interactions. J Biol Chem 2016;291:12627–12640.
26 Lee RH, Pulin AA, Seo MJ et al. Intravenous hMSCs improve myocardial infarction in mice because cells embolized in lung are activated to secrete the anti-inflammatory protein TSG-6. Cell Stem Cell 2009;5:54–63.
27 Lee RH, Yu JM, Foskett AM et al. TSG-6 as a biomarker to predict efficacy of human mesenchymal stem/progenitor cells (hMSCs) in modulating sterile inflammation in vivo. Proc Natl Acad Sci USA 2014;111:16766–16771.
28 He Z, Hua J, Qian D et al. Intravenous hMSCs ameliorate acute pancreatitis in mice via secretion of tumor necrosis factor-alpha stimulated gene/protein 6. Sci Rep 2016;6: 38438.
29 Qi Y, Jiang D, Sindrilaru A et al. TSG-6 released from intradermally injected mesenchymal stem cells accelerates wound healing and reduces tissue fibrosis in murine full-thickness skin wounds. J Invest Dermatol 2014;134: 526–537.
30 Sala E, Genua M, Petti L et al. Mesenchymal stem cells reduce colitis in mice via release of TSG6, independently of their localization to the intestine. Gastroenterology 2015; 149:163.e120–176.e120.
31 Nikolopoulos SN, Turner CE. Actopaxin, a new focal adhesion protein that binds paxillin LD motifs and actin and regulates cell adhesion. J Cell Biol 2000;151:1435–1448.
32 Lee E, De Camilli P. Dynamin at actin tails. Proc Natl Acad Sci USA 2002;99:161–166.
33 Phinney DG, Pittenger MF. Concise review: MSC-derived exosomes for cell-free therapy. Stem Cells 2017;35:851–858.
34 Friedenstein AJ. Stromal mechanisms of bone marrow: Cloning in vitro and retransplantation in vivo. Haematol Blood Transfus 1980;25:19–29.
35 Almalki SG, Agrawal DK. Key transcription factors in the differentiation of mesenchymal stem cells. Differentiation 2016;92: 41–51.
36 Mahoney DJ, Mulloy B, Forster MJ et al. Characterization of the interaction between tumor necrosis factor-stimulated gene-6 and heparin: Implications for the inhibition of plasmin in extracellular matrix microenvironments. J Biol Chem 2005;280:27044–27055.
37 Park Y, Jowitt TA, Day AJ et al. Nuclear magnetic resonance insight into the multiple glycosaminoglycan binding modes of the link module from human TSG-6. Biochemistry 2016;55:262–276.
38 Melendez J, Liu M, Sampson L et al. Cdc42 coordinates proliferation, polarity, migration, and differentiation of small intestinal epithelial cells in mice. Gastroenterology 2013;145:808–819.
39 Garlanda C, Bottazzi B, Magrini E et al. PTX3, a humoral pattern recognition molecule, in innate immunity, tissue repair, and cancer. Physiol Rev 2018;98:623–639.
40 Djouad F, Charbonnier LM, Bouffi C et al. Mesenchymal stem cells inhibit the differentiation of dendritic cells through an interleukin-6-dependent mechanism. Stem Cells 2007;25: 2025–2032.
41 Rincon M. Interleukin-6: From an inflammatory marker to a target for inflammatory diseases. Trends Immunol 2012;33:571–577.
42 Bromberg J, Wang TC. Inflammation and cancer: IL-6 and STAT3 complete the link. Cancer Cell 2009;15:79–80.
43 Grivennikov S, Karin M. Autocrine IL-6 signaling: A key event in tumorigenesis? Cancer Cell 2008;13:7–9.
44 Heikkila K, Ebrahim S, Lawlor DA. Systematic review of the association between circulating interleukin-6 (IL-6) and cancer. Eur J Cancer 2008;44:937–945.
45 Lippitz BE. Cytokine patterns in patients with cancer: A systematic review. Lancet Oncol 2013;14:e218–e228.
46 Li W, Zhou Y, Yang J et al. Gastric cancer-derived mesenchymal stem cells prompt gastric cancer progression through secretion of interleukin-8. J Exp Clin Cancer Res 2015; 34:52.
47 Scherzad A, Steber M, Gehrke T et al. Human mesenchymal stem cells enhance cancer cell proliferation via IL-6 secretion and activation of ERK1/2. Int J Oncol 2015;47: 391–397.
48 Becker C, Fantini MC, Wirtz S et al. IL-6 signaling promotes tumor growth in colorectal cancer. Cell Cycle 2005;4:217–220.
49 Zhang X, Liu S, Zhou Y. Circulating levels of C-reactive protein, interleukin-6 and tumor necrosis factor-alpha and risk of colorectal adenomas: A meta-analysis. Oncotarget 2016; 7:64371–64379.
50 Djouad F, Plence P, Bony C et al. Immunosuppressive effect of mesenchymal stem cells favors tumor growth in allogeneic animals. Blood 2003;102:3837–3844.
51 Galie M, Konstantinidou G, Peroni D et al. Mesenchymal stem cells share molecular signature with mesenchymal tumor cells and favor early tumor growth in syngeneic mice. Oncogene 2008;27:2542–2551.
52 Mathew E, Brannon AL, Del Vecchio A et al. Mesenchymal stem cells promote pancreatic tumor growth by inducing alternative polarization of macrophages. Neoplasia 2016; 18:142–151.
53 Spaeth EL, Dembinski JL, Sasser AK et al. Mesenchymal stem cell transition to tumor-associated fibroblasts contributes to fibrovascular network expansion and tumor progression. PLoS One 2009;4:e4992.
54 Yu JM, Jun ES, Bae YC et al. Mesenchymal stem cells derived from human adipose tissues favor tumor cell growth in vivo. Stem Cells Dev 2008;17:463–473.
55 Mandel K, Yang Y, Schambach A et al. Mesenchymal stem cells directly interact with breast cancer cells and promote tumor cell growth in vitro and in vivo. Stem Cells Dev 2013;22:3114–3127.
56 Piccinato CA, Sertie AL, Torres N et al. High OCT4 and low p16(INK4A) expressions determine in vitro lifespan of mesenchymal stem cells. Stem Cells Int 2015;2015:369828.
57 Freund A, Laberge RM, Demaria M et al. Lamin B1 loss is a senescence-associated biomarker. Mol Biol Cell 2012;23:2066–2075.
58 Coulson-Thomas VJ, Lauer ME, Soleman S et al. Tumor necrosis factor-stimulated gene-6 (TSG-6) is constitutively expressed in adult central nervous system (CNS) and associated with astrocyte-mediated glial scar formation

following spinal cord injury. J Biol Chem 2016; 291:19939–19952.
59 Lawrance W, Banerji S, Day AJ et al. Binding of hyaluronan to the native lymphatic vessel endothelial receptor LYVE-1 is critically dependent on surface clustering and hyaluronan organization. J Biol Chem 2016; 291:8014–8030.
60 Wang Y, Yago T, Zhang N et al. Cytoskeletal regulation of CD44 membrane organization and interactions with E-selectin. J Biol Chem 2014;289:35159–35171.
61 Freeman SA, Vega A, Riedl M et al. Transmembrane pickets connect cyto- and pericellular skeletons forming barriers to receptor engagement. Cell 2018;172:305. e310–317.e310.
62 Christianson HC, Belting M. Heparan sulfate proteoglycan as a cell-surface endocytosis receptor. Matrix Biol 2014;35:51–55.
63 Sipes NS, Feng Y, Guo F et al. Cdc42 regulates extracellular matrix remodeling in three dimensions. J Biol Chem 2011;286: 36469–36477.
64 Humphrey JD, Dufresne ER, Schwartz MA. Mechanotransduction and extracellular matrix homeostasis. Nat Rev Mol Cell Biol 2014;15:802–812.
65 Darnell M, O'Neil A, Mao A et al. Material microenvironmental properties couple to induce distinct transcriptional programs in mammalian stem cells. Proc Natl Acad Sci USA 2018;115:E8368–E8377.
66 Cary LA, Guan JL. Focal adhesion kinase in integrin-mediated signaling. Front Biosci 1999;4:D102–D113.
67 Guo XR, Ding SL, Pan XQ et al. Expression of TSG-6 gene during 3T3-L1 preadipocyte differentiation and regulative role of tumor necrosis factor-alpha. Zhonghua Er Ke Za Zhi 2004;42:344–347.
68 Dominici M, Le Blanc K, Mueller I et al. Minimal criteria for defining multipotent mesenchymal stromal cells. The International Society for Cellular Therapy position statement. Cytotherapy 2006;8:315–317.
69 Fisher DT, Appenheimer MM, Evans SS. The two faces of IL-6 in the tumor microenvironment. Semin Immunol 2014;26:38–47.
70 Pricola KL, Kuhn NZ, Haleem-Smith H et al. Interleukin-6 maintains bone marrow-derived mesenchymal stem cell stemness by an ERK1/2-dependent mechanism. J Cell Biochem 2009;108:577–588.
71 Rattigan Y, Hsu JM, Mishra PJ et al. Interleukin 6 mediated recruitment of mesenchymal stem cells to the hypoxic tumor milieu. Exp Cell Res 2010;316:3417–3424.
72 Mi F, Gong L. Secretion of interleukin-6 by bone marrow mesenchymal stem cells promotes metastasis in hepatocellular carcinoma. Biosci Rep 2017;37:BSR20170181.
73 Xu H, Zhou Y, Li W et al. Tumor-derived mesenchymal-stem-cell-secreted IL-6 enhances resistance to cisplatin via the STAT3 pathway in breast cancer. Oncol Lett 2018;15: 9142–9150.
74 Barcellos-de-Souza P, Comito G, Pons-Segura C et al. Mesenchymal stem cells are recruited and activated into carcinoma-associated fibroblasts by prostate cancer microenvironment-derived TGF-beta1. Stem Cells 2016;34:2536–2547.
75 Prantl L, Muehlberg F, Navone NM et al. Adipose tissue-derived stem cells promote prostate tumor growth. Prostate 2010;70: 1709–1715.
76 Suzuki K, Sun R, Origuchi M et al. Mesenchymal stromal cells promote tumor growth through the enhancement of neovascularization. Mol Med 2011;17:579–587.
77 He N, Kong Y, Lei X et al. MSCs inhibit tumor progression and enhance radiosensitivity of breast cancer cells by down-regulating Stat3 signaling pathway. Cell Death Dis 2018; 9:1026.
78 Khakoo AY, Pati S, Anderson SA et al. Human mesenchymal stem cells exert potent antitumorigenic effects in a model of Kaposi's sarcoma. J Exp Med 2006;203:1235–1247.
79 Pacioni S, D'Alessandris QG, Giannetti S et al. Human mesenchymal stromal cells inhibit tumor growth in orthotopic glioblastoma xenografts. Stem Cell Res Ther 2017;8:53.
80 Ramasamy R, Lam EW, Soeiro I et al. Mesenchymal stem cells inhibit proliferation and apoptosis of tumor cells: Impact on in vivo tumor growth. Leukemia 2007;21: 304–310.
81 Zhu Y, Sun Z, Han Q et al. Human mesenchymal stem cells inhibit cancer cell proliferation by secreting DKK-1. Leukemia 2009; 23:925–933.
82 Dvorak HF. Tumors: Wounds that do not heal. Similarities between tumor stroma generation and wound healing. N Engl J Med 1986;315:1650–1659.


See www.StemCells.com for supporting information available online.

